14 August 1981, Volume 213, Number 4509 SCIENCE

Phonon Optics and Phonon Propagation in Semiconductors

V. Narayanamurti

Acoustic waves or sound waves result from the vibrations of atoms or molecules and at audible frequencies (lower than about 20 kilohertz) can be generated in many different ways. Human speech, for example, lies in this range. Sound waves at these frequencies can propagate reasonably well through the atmosphere, as evidenced by the fact that the waves can be heard from afar. But at higher frequencies (about 1 megahertz), where sound waves are inaudible, the atmosphere is a poor medium for propagation; ultrasonic waves are rapidly dissipated in the gases of the air and can be made to travel appreciable distances only in condensed media such as liquids and solids. Acoustic waves vibrating in condensed matter at ultrasonic frequencies are usually generated by radio-frequency excitation of piezoelectric materials such as quartz.

Summary. Recent experiments involving the propagation of extremely high frequency, short-wavelength acoustic phonons in semiconductors are described. Such phonons, which play an important role in thermal energy transport and nonradiative recombination processes, can be used as sensitive microscopic probes of electronic, defect, and interface states. Experiments on phonon transmission through epitaxially grown bulk material as well as thin-film superlattice structures in the semiconductor gallium arsenide are described. Such thin-film periodic structures can be used to build frequency-selective phonon filters and reflectors, which can in turn be used to manipulate phonon diagnostic beams in technologically important materials.

In the megahertz region ultrasonic waves have been widely used for the study of underwater objects, internal structural features in materials, and even organs inside the human body. The wavelength of megahertz ultrasonic waves in many solids is typically in the millimeter region, and thus such waves are sensitive to features that are macroscopic in size. Using microwave (*1*) excitation of piezoelectric thin films or surfaces, one can extend the frequency to the gigahertz (10^9 Hz) regime and the wavelength can be reduced to the submicrometer region. Since the early 1960's microwave ultrasonics has been widely used for the study of materials (*2*). Recently, an ultrasonic imaging apparatus, the acoustic microscope, was developed by Quate (*3*) to generate "acoustic pictures" with a resolution comparable to that of visible light microscopy. Sound waves and light waves are reflected and absorbed differently by the same object and thus can often yield complementary microscopic information about the materials being studied.

Acoustic propagation (*4*) experiments with conventional piezoelectric transducers become quite difficult at frequencies beyond about 10^{10} Hz. Sound waves with frequencies of hundreds of gigahertz and terahertz (10^{12} Hz) are well into the thermal vibrational spectrum of the solid. At these enormously high frequencies the discrete nature of the spectrum becomes important, and the quantized lattice vibrations—also referred to as phonons—have extremely short wavelengths, in the range 10 to 100 angstroms. Because of the short wavelength it becomes extremely difficult to preserve the phase coherence of a piezoelectrically generated wave as it traverses the boundary between the generator and the transmission medium under study. In addition, propagation of such high-frequency phonons can be severely affected by the presence of defects and by phonon-phonon scattering.

The problem of preserving the phase coherence of high-frequency phonons as they traverse the generator-sample boundary can be circumvented through the use (*5*) of an incoherent source such as a thin (~1000 Å) metal film, which can be vacuum-deposited and forms an excellent "bond" with the crystalline medium under study. In the case of a normal metal film such as gold or copper, the resistive heating results in a broad Planck frequency distribution (see Fig. 1a) with a peak in frequency that depends on the temperature, T_h, of the heater. For a value of $T_h \sim 10$ K the peak phonon frequency is ~0.6 THz. Such metal heaters are thus efficient sources of high-frequency phonons, but have a broad distribution similar to tungsten lamps in optics. The heat-generated phonons can be detected at the other end of the sample by means of a sensitive thin-film bolometer, that is, a device whose resistance is a strong function of temperature.

In order to get a more monochromatic distribution of high-frequency phonons one has to make use of the detailed quantum mechanical interaction between electrons and phonons in metals or semiconductors. In the case of superconductors, the existence of the energy gap, 2Δ, leads to the possibility that phonons can excite electrons across the gap, in analogy with the photoelectric effect. A superconducting device that can be used to generate high-frequency phonons is shown on the left side of Fig. 1b and is known as a tunnel junction. It consists of a sandwich of extremely thin (~ 1000 Å) films of two superconductors with an insulator (~ 20 Å) in between. When a voltage, V, is applied across the sandwich, the insulator acts as a gate that transmits only electrons of energy

The author is head of the Semiconductor Electronics Research Department, Bell Laboratories, Murray Hill, New Jersey 07974.

0036-8075/81/0814-0717$01.00/0

Table 1. Transition temperature T_c, energy gap 2Δ, and gap frequency $\nu = \omega/2\pi$ for several superconductors.

Superconductor	T_c (K)	2Δ (meV)	ν (10^{11} Hz)
Al	1.18	0.36	0.9
Sn	3.8	1.2	2.9
Pb	7.2	2.7	6.7
$Pb_{0.85}Bi_{0.15}$	8.5	3.2	8.0

$eV > 2\Delta$, where e is the electron charge. The injected electrons transfer their energy to the lattice in the form of phonons with a spectral distribution that strongly deviates from a thermal Planck distribution. For voltages close to a value such that $eV = 2\Delta$, the recombination radiation corresponds to phonons of frequency $\nu = 2\Delta/h$. For higher voltages "relaxation" phonons of energy $eV - 2\Delta$ can also be emitted. Thus the phonon spectrum depends in a characteristic way on the electron injection energy. The upper frequency limit of the relaxation phonon spectrum is determined by reabsorption processes in the superconducting film, and in favorable cases (*6*) it can exceed the superconducting energy gap. Table 1 shows the transition temperature, T_c, and zero-temperature energy gap for a few common superconductors. It is clear that quantum processes in superconductors can be used for the generation and detection of phonons (*6*) in the range 10^{11} to 10^{12} Hz.

Scope of This Article

Besides thin metal film transducers one can, in the case of semiconductors, use the electronic energy states of donors, acceptors, and other atomic defects, which, when preferentially excited either electrically or by optical means, can lose their energy by phonon processes (*7*). Thus phonon transport experiments are an extremely useful means of studying nonradiative energy transport. Such nonradiative processes contribute to losses in a variety of technologically important luminescent devices. With semiconductors such as GaAs one can use novel epitaxially grown transducer materials, which are lattice-matched to the transmitting medium so that interfacial defect degradation is negligible. Thus nonradiative recombination in *pn* junctions and epitaxial *n*- and *p*-type layers of controlled doping can be studied. In addition, the transmission of phonons through epitaxially grown layered material can be studied with conventional superconducting tunnel junction generators and detectors (see Fig. 2). One can, for example, by means of molecular beam epitaxy (MBE), grow superlattice structures (*8*) with a controlled period. These structures can be used to build frequency-selective phonon filters and reflectors, which can in turn be used to manipulate phonon beams. Such manipulation of phonons with novel transducer materials and the physical studies made possible by this means may best be described as "phonon optics" and are the subject of this article.

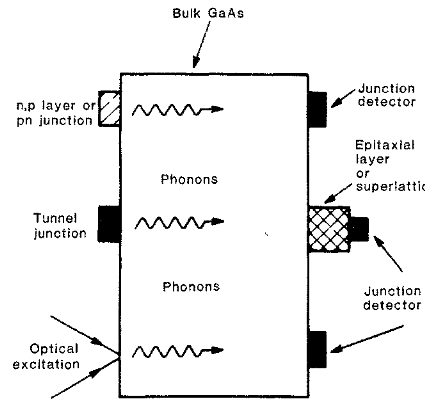

Fig. 2. Experimental arrangement for phonon propagation in a bulk semiconductor such as GaAs. Phonons may be generated by optical excitation or by means of an epitaxial *n,p* layer or *pn* junction. Transmission through an epitaxial layer or superlattice can be studied with conventional tunnel junction generators and detectors.

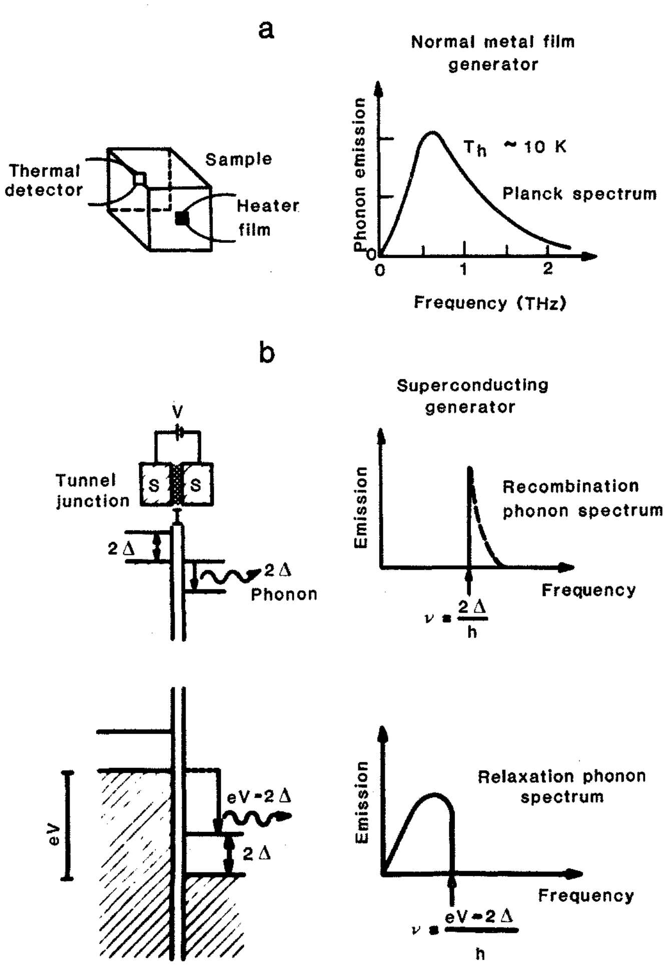

Fig. 1. (a) Schematic of experimental arrangement with thin metal film transducers. Emission spectrum for a normal metal film for a characteristic temperature of 10 K. (b) Spectrum of phonons generated by a superconducting tunnel junction generator under different conditions of bias.

Ballistic Propagation and Phonon Focusing

Propagation of heat in most materials is generally thought to be a slow diffusive process. This is true if the phonons that carry the heat suffer frequent scattering events. These scattering events are usually the result of the presence of defects and free carriers and of intrinsic phonon-phonon interactions. Phonon-phonon interactions can be minimized by cooling the sample to low temperatures when the population of thermally excited phonons is small. In "perfect" dielectric solids and semiconductors at low temperatures heat propagation can thus be ballistic; that is, the phonons created by a pulse of heat at one point can travel rectilinearly for distances of the order of centimeters at the velocity of sound. Such ballistic propagation of heat was first observed by Von Gutfeld and Nethercot (*9*).

Figure 3a shows typical heat pulses (*10*) observed in the <110>, <111>, and

<100> crystallographic directions in pure GaAs for an almost identical propagation length of about 2.5 millimeters. The separate pulses correspond to ballistic traversal of longitudinal (L) and fast and slow transverse (FT and ST, respectively) phonons, whose velocity depends on the direction of phonon propagation. The longitudinal mode is a compression wave and has the highest velocity. The transverse modes are primarily shear waves and have a lower velocity. The two shear waves in the <111> and <100> directions have the same velocity. It is also clear from Fig. 3a that the relative intensity of the T and L pulses changes by more than an order of magnitude depending on the orientation. It is ~ 1 in the <111> direction and ~ 20 in the <100> direction. This focusing of the phonon intensity is due to the elastically anisotropic nature of the solid and was first observed in heat pulse experiments by Taylor *et al.* (*11*). In anisotropic crystals the phase velocity $v = \omega(\mathbf{k})/|\mathbf{k}|$ depends on the direction of the wave vector **k** and can be calculated (*12*) from the constant-frequency or "slowness" surface $\omega(\mathbf{k})$ = constant. This surface is shown for the slow transverse mode in GaAs in Fig. 3b. The group velocity, $v_g = \partial\omega(\mathbf{k})/\partial\mathbf{k}$, which defines the direction of energy flow, is also very anisotropic. A cross section of the slowness surface and the directions of the energy flow for the [100] plane are shown in Fig. 3c. In this case the energy flow is strongly enhanced or focused along the [100], [010], and [001] symmetry axes, which explains the high T-mode intensities relative to the L mode observed in the <100> direction in Fig. 3a.

The focusing of phonon beams can be numerically calculated from a three-dimensional slowness surface such as that shown in Fig. 3b. Maris (*13*) showed that the energy flux enhancement, A, is determined by the ratio of the solid angles in **k** space and energy flux or ray (**r**) space: $A = d\Omega^k/d\Omega^r$. For a spherical surface $A = 1$. For an anisotropic surface A can be calculated from a knowledge of the Gaussian curvature, K, as shown by Lighthill (*14*), Lax and Narayanamurti (*15*), and Rösch and Weis (*16*). The Gaussian curvature for a two-dimensional surface element is simply the product of the two principal curvatures (inverse radii) of the element. The magnification A is inversely proportional to K. It is possible for K to equal zero along certain directions; this depends on the topology of the $\omega(\mathbf{k}) = \omega$ surface. Whenever K equals zero the magnification A would be infinite, and one would actually have a focusing singularity.

The presence of singular points, where $K = 0$, was demonstrated in a high-resolution heat pulse experiment in crystalline germanium by Hensel and Dynes (*17*). They devised a method for monitoring the heat pulse intensities as the direction of propagation was changed continuously. An extremely small aluminum superconducting bolometer was used as a detector, and the heat pulses were generated by pulsed laser excitation of a metal film evaporated on the cylindrical surface of the rotatable germanium sample. Figure 4a shows the angular distribution of measured T-mode intensities in the [110] plane. Sharp intensity jumps in the vicinity of the <100> and <110> directions are observed, and the results are in excellent agreement with theoretical computations of K and A for the material.

By using an x-y laser scanning system, Northrup and Wolfe (*18*) reconstructed a three-dimensional pattern of focused

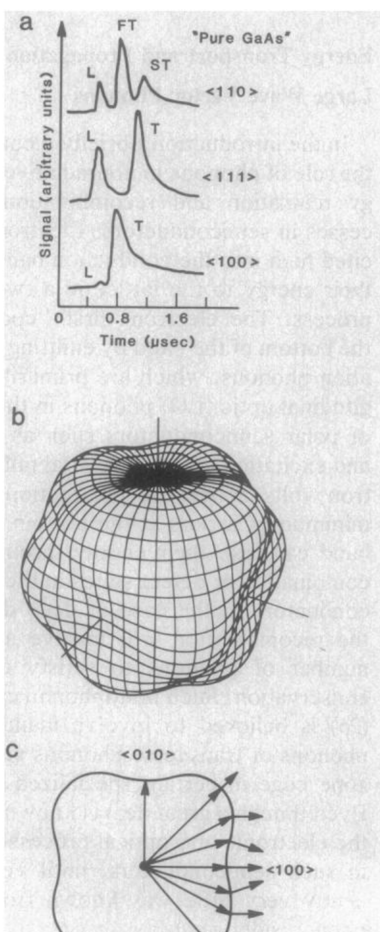

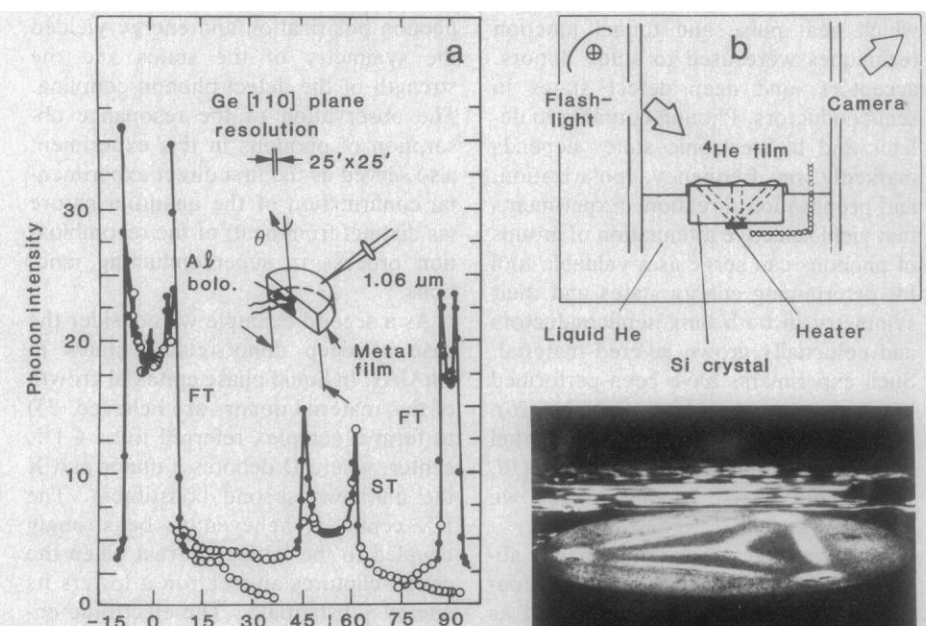

Fig. 3 (left). (a) Ballistic phonons in "pure" GaAs for three different propagation directions; propagation length, ~ 2.3 mm. (b) Constant-frequency surface for the slow transverse mode in GaAs. (c) Cross section of the same surface in the [100] plane and showing the focusing of the energy flux. Fig. 4 (right). (a) Angular dependence of phonon focusing in germanium in the [110] plane. The peaks around 0° and 90° are due to fast transverse (*FT*) modes, those around 45° to slow transverse (*ST*) modes. After Hensel and Dynes (*17*). (b) Experimental arrangement for photographing the focusing of heat pulses in silicon. The photograph at the bottom shows the observed heat flux pattern for a ⟨111⟩ viewing direction. After Eisenmenger (*19*).

phonons in germanium in the form of a photograph. Eisenmenger (19) developed a novel method for imaging such focused phonons. In his experimental arrangement (Fig. 4b) a large single crystal of silicon was used. It had a thin-film heater on one side and was partially immersed in a bath of superfluid helium at 1.5 K, with the top surface covered with a film of the superfluid. When the heater was turned on, superfluid flowed to the hotter regions and the film thickness was locally increased. These changes in film thickness were photographed with a camera. A typical pattern observed by Eisenmenger is shown at the bottom of Fig. 4b. The threefold symmetry of the heated regions is consistent with the <111> direction of the crystal used and with theoretical computations. The focusing of phonon beams influences all ballistic phonon experiments in crystals. Detailed knowledge of this phenomenon is essential for all quantitative experiments involving the coupling of phonons to electrons and to defects in semiconductors.

Phonon-Defect Interactions in Semiconductors

A great deal of work has been done in which heat pulse and tunnel junction techniques were used to study donors, acceptors, and deep defect states in semiconductors. Phonon coupling to defects and to electronic states depends markedly on frequency, polarization, and propagation direction. Experiments that yield selective attenuation of groups of phonons can serve as a valuable tool for determining energy states and their symmetry in both bulk semiconductors and epitaxially grown layered material. Such experiments have been performed by Pomerantz and Von Gutfeld (20), Dynes and Narayanamurti (21), Forkel *et al.* (22), and Narayanamurti *et al.* (10, 23) among others. In this section we consider two illustrative examples.

The first direct phonon resonance absorption experiment in which superconducting tunnel junctions were used as sources and detectors of "quasimonochromatic" phonons was performed by Dynes *et al.* (24). They used the pressure dependence of the energy levels of the shallow donor antimony in germanium to obtain a resonance absorption of 2Δ phonons generated by a superconducting tin tunnel junction. In Fig. 5a we show a schematic of the experimental arrangement as well as the theoretically predicted variation of the energy levels as a function of uniaxial pressure applied

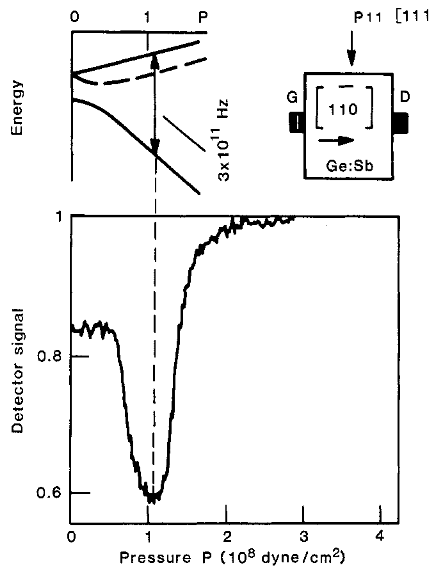

Fig. 5. Transmission of 1.2-meV phonons through an ~ 4 mm thick sample of germanium doped with about 2×10^{15} antimony donors as a function of uniaxial pressure (24).

along the ⟨111⟩ direction. The generator was biased at a voltage $eV = 2\Delta = 1.2$ meV so that only recombination radiation was emitted by the junction. At a value of stress corresponding to an energy splitting of 1.2 meV a strong decrease in the phonon transmission was observed. Measurements as a function of phonon polarization and energy yielded the symmetry of the states and the strength of the defect-phonon coupling. The observation of the resonance absorption of phonons in this experiment also served as the first direct experimental confirmation of the quantum nature (as distinct from heat) of the recombination process in superconducting junctions.

As a second example we consider the case of deep donor-related states in GaAlAs. In liquid phase epitaxial growth of this material donors are believed (25) to form a complex referred to as a DX center, where D denotes a donor and X the unknown second constituent. The DX center is believed to be strongly coupled to the lattice, so that when the center captures an electron it lowers its energy substantially. The electronic energy is shown as a function of the lattice configuration, Q, on the right side of Fig. 6a. The center can be emptied (ionized) by optical excitation at energy E_{opt}. The combined effect of the electron-lattice coupling and the defect potential produces a bound state when the defect is occupied.

Direct experimental confirmation of the strong defect-lattice coupling and the symmetry of the DX centers was obtained for the first time by ballistic phonon attenuation techniques (23). The donors used in the experiments were either tellurium (which takes the place of arsenic in the lattice) or tin (which takes the place of gallium). A thick (~ 2.5 mm) sample of GaAs was used as a transmitting medium, on one end of which was grown a $Ga_{0.5}Al_{0.5}As$ expitaxial layer of typical thickness 10 micrometers. Doped and undoped layers were grown side by side so that the effects of doping could be monitored. Photoexcitation by means of a flash lamp was used to change the occupation of the DX centers in situ in the expitaxial layers. The propagation direction was ⟨110⟩.

Figure 6 also shows typical ballistic pulses observed in the dark and after photoexcitation. In the case of tin donors strong attenuation of FT modes was observed while attenuation of the ST mode was negligible. In the case of tellurium donors both T modes suffered attenuation. From group theoretical arguments (2) the selective attenuation was interpreted (23) as arising from trigonal centers in the case of tin doping and orthorhombic centers in the case of tellurium doping. This measurement has been particularly useful, as other diagnostic techniques such as electron spin resonance are difficult to use in this system.

Energy Transport and Propagation of Large Wave Vector Phonons

In the introduction I briefly mentioned the role of phonons in nonradiative energy relaxation and recombination processes in semiconductors. Electrons excited high into the conduction band lose their energy to the lattice in a two-step process. The electrons first "cool" to the bottom of the band by emitting relaxation phonons, which are primarily longitudinal optic (LO) phonons in the case of polar semiconductors such as GaAs and excitation energies several millielectron volts above the conduction band minimum. Carriers at the bottom of the band can lose their energy through recombination at defect states in the semiconductor. In the case of deep defects the recombination will involve a large number of phonons to satisfy energy conservation. Such multiphonon capture (26) is believed to involve mainly LO phonons or transverse phonons near the zone edge in certain specialized cases. Even though a great deal is known about the electronic and optical processes (27) in such semiconductors, until very recently very little was known from the phonon side.

Figure 7 shows some results on phonon generation after photoexcitation (28) in GaAs. A tunable, pulsed dye laser capable of operating at wavelengths above the band gap of GaAs was used for the photoexcitation. The phonon detector was a lead oxide–lead superconducting tunnel junction with a frequency threshold of about 0.7 THz. In most directions of propagation, which could be varied in situ in the experiment, besides the direct optical luminescent pickup at $t = 0$ a single broad transverse pulse was observed. These results are to be compared with the sharp pulses observed with metal film generators shown in Fig. 3a. The arrival time of the leading edge and half-height and peak of the pulse scaled linearly with the propagation distance for distances of several millimeters. Detailed studies of the shape of the pulse showed that it could be described as consisting of ballistically propagated phonons with a considerable spread in velocity. For example, the velocity corresponding to the peak of the pulse was $\sim 0.7 \times 10^5$ centimeters per second for the ⟨111⟩ direction of propagation, but the low-frequency ballistic velocity in this direction is 2.8×10^5 cm/sec.

These data can be interpreted from a knowledge of the phonon dispersion curves (29) of frequency ω versus wave vector $\mathbf{k}$. Such a curve for different polarization branches of GaAs, as determined by neutron scattering, is shown in Fig. 8. The curves correspond to the LO, longitudinal acoustic (LA), and transverse acoustic (TA) branches. Optically excited electron-hole (e-h) pairs lose a substantial portion of their energy by emission of LO phonons. These phonons in turn quickly decay (in $\sim 10^{-11}$ second) into lower-lying LA and TA branches. Because the decay processes require simultaneous conservation of energy and momentum ($\hbar\omega = \hbar\omega_1 + \hbar\omega_2$, $\mathbf{k} = \mathbf{k}_1 + \mathbf{k}_2$, where $\hbar$ is Planck's constant divided by 2π) most of the energy ends up in the lowest TA branch which, because of the bending of the phonon dispersion curve at large wave vectors, cannot decay (30) any further. These ultrashort-wavelength phonons (~ 10 Å) correspond to phonons well into the Brillouin zone of the crystal and have a group velocity $d\omega/dk$ much less than the low-frequency ultrasonic velocity. The stippled area shows the regime of superconducting tunnel junction phonon spectroscopy.

These experiments show that nonradiative recombination in semiconductors occurs through phonons with large wave vectors, some of which are able to propagate macroscopic distances ($\sim$ millimeters) through the semiconductor. The properties of such ultrashort-wavelength phonons are quite different from those of low-frequency ones, which correspond to continuum elasticity theory. Because of the dispersion in phonon velocity at short wavelengths and the observed long mean free paths, time-resolved spectroscopy has been used for velocity selection of phonons (31) of different wavelengths and to study scattering as a function of wavelength. Such experiments provide a valuable diagnostic tool for defect and electronic energy states in semiconductors.

The Phonon Mirror

As a final example (32) I describe a novel thin-film spectrometer based on the selective filtering action of an acoustic superlattice of GaAs and AlGaAs. This has been made possible through the use of MBE growth techniques (8). Because of the technological importance of GaAs, a great deal of effort has been spent to grow nearly perfect superlattice structures based on the GaAs/AlGaAs system. Because of its artificial periodicity, such a superlattice can serve as a frequency-selective phonon mirror or fil-

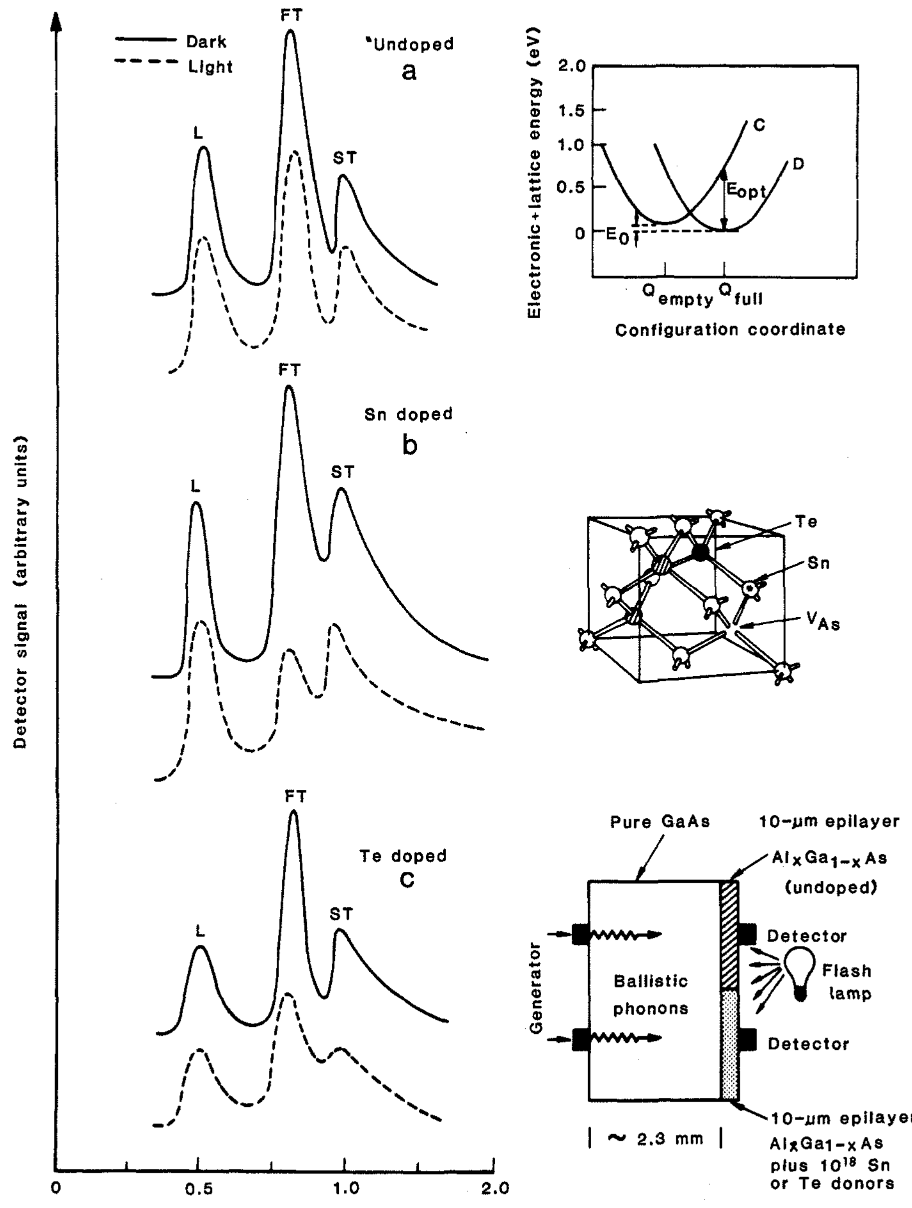

Fig. 6. Ballistic phonon intensities for three different samples of $Al_{0.5}Ga_{0.5}As$. (a) Nominally undoped material, (b) with $\sim 10^{18}$ Sn donors per cubic centimeter, and (c) with $\sim 10^{18}$ Te donors per cubic centimeter. Solid lines are data taken in the dark; dashed lines are data taken after photoexcitation. The propagation direction is ⟨110⟩. The intensities of the ballistic phonons reveal selective attenuation of certain groups of transverse modes depending on the symmetry of the donor-related photoconductivity center. The right-hand side of (a) shows a typical configuration-coordinate diagram for such centers. A crystal model of GaAs and a schematic of the experimental arrangement are also shown in (b) and (c) (23).

ter. The filtering action arises from selective reflection by the superlattice of phonons of wavelength λ_0 that fulfill the Bragg condition $\lambda_0 = 2d$, where d is the superlattice period (*33*). In view of the close analogy with optical dielectric mirrors, an appropriately designed thin-film heterostructure superlattice may be called a dielectric phonon mirror. Besides the frequency selectivity, one of the most significant results is the observation that high-frequency phonons pass through the more than 100 interfaces of the multilayer structure without significant degradation.

The reflection of phonons propagating normal to the interface between two elastic media of different acoustical impedances Z_1 and Z_2 is analogous to the reflection of electromagnetic waves at the interface between two optical media with different indices of refraction n_1 and n_2. To calculate the phonon transmission properties of a multilayer stack, we followed the mathematical procedures outlined in classical optics textbooks (*34*). The acoustic properties of each semiconductor layer are expressed in terms of a characteristic matrix. The superlattice is then described as an equivalent layer and

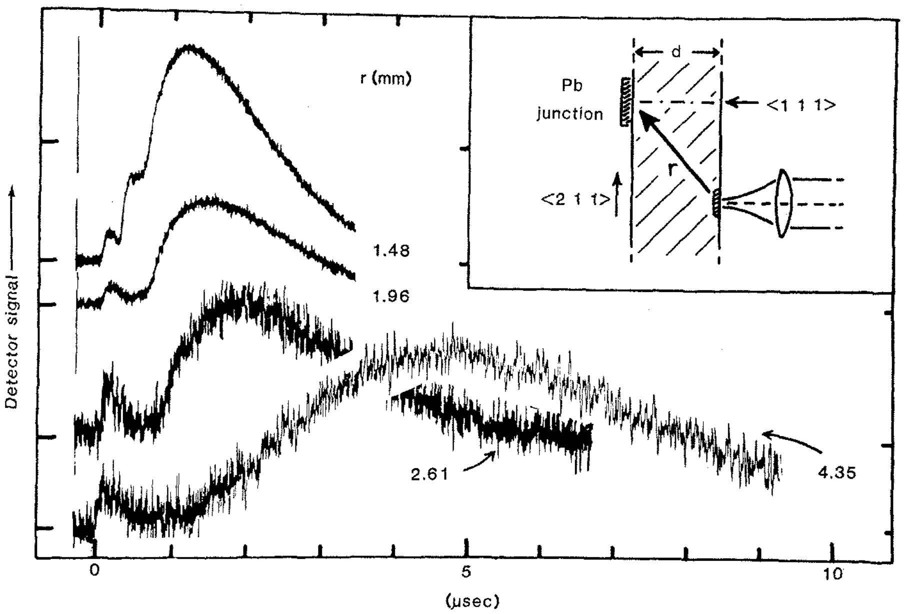

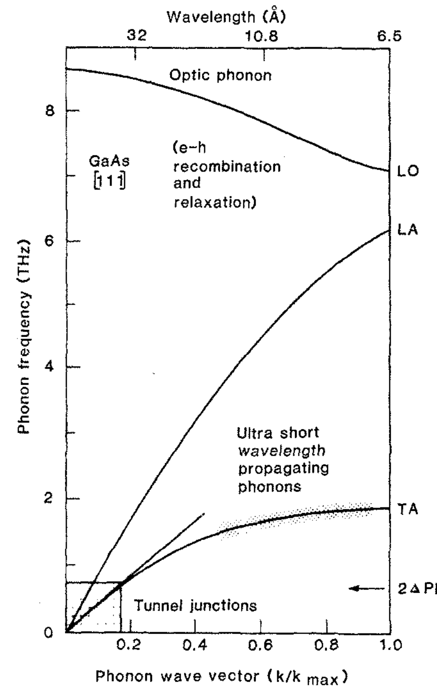

Fig. 7 (left). Phonon generation due to nonradiative recombination in optically excited GaAs. A lead junction detector was used. Signals are shown as a function of time for several different propagation distances. The signal at zero time is due to optical luminescent pickup (*28*). Fig. 8 (right). Phonon dispersion curves for GaAs [111]. Optic phonons generated during e-h recombination and relaxation decay into the lowest TA branch, which is unable to decay any further.

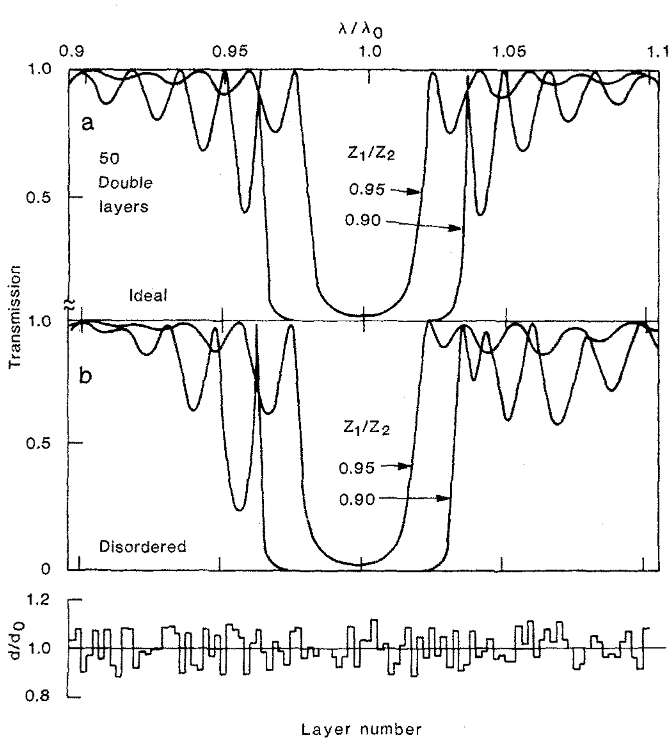

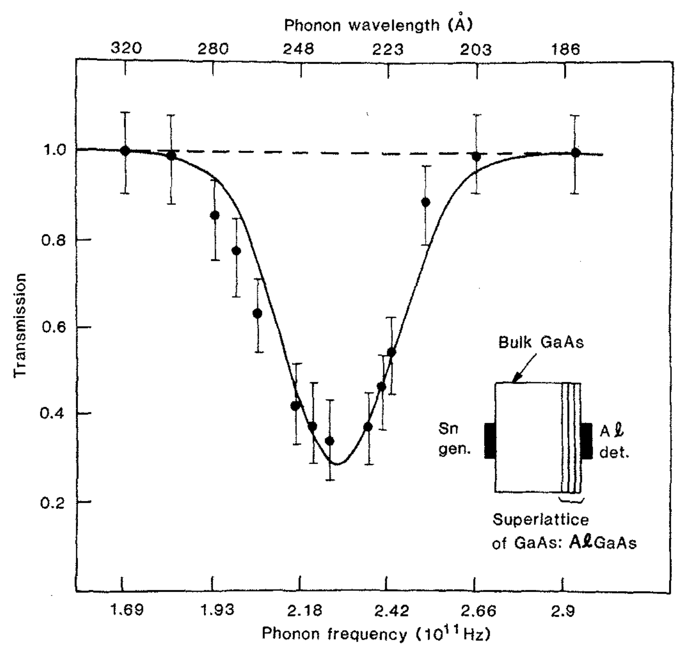

Fig. 9 (left). Theoretical calculation of the transmission of acoustic waves for a multilayer stack of 50 layers and acoustic impedance ratio Z_1/Z_2 of 0.95 and 0.90. (a) Ideal superlattice; (b) superlattice with 10 percent disorder in thickness as shown in the trace at bottom (*32*). Fig. 10 (right). Phonon transmission through a $GaAs/Al_{0.5}Ga_{0.5}As$ superlattice of period 122 Å and 50 double layers. Dots correspond to experimental points and the solid line corresponds to a theoretical fit for an acoustic impedance ratio Z_1/Z_2 of 0.88 and an overall line width of $\sim 0.24 \times 10^{11}$ Hz (*32*).

its matrix is a product of the characteristic matrices of the individual layers, from which transmission and reflection coefficients can be readily derived. Through individual matrix multiplication one can investigate the influence of layer thickness fluctuations and of systematic error in the relative thickness of GaAs and AlGaAs (due to sound velocity uncertainties) on the reflection properties of the stack.

Figure 9a shows the transmission for an ideal superlattice of 50 layer pairs of $GaAs/Al_xGa_{1-x}As$ of individual layer thickness $\lambda_0/4$ for two different values of Z_1/Z_2. The ratio Z_1/Z_2 is believed to be around 0.90 for $x = 0.5$. Figure 9b gives the result of the same calculation with allowance for a random thickness variation of each individual layer of ± 10 percent, which is the upper limit of the disorder we might expect in samples grown by MBE. Comparison of Fig. 9, a and b, shows that this degree of disorder only slightly degrades the reflection properties of the acoustic superlattice. Calculations that included sound velocity uncertainties of up to 10 percent had practically no additional influence on the line width.

The inset of Fig. 10 shows a schematic of the experimental arrangement used to test some of these ideas. An Sn tunnel junction is used as a source of phonons, which pass through a $GaAs/Al_{0.5}Ga_{0.5}As$ superlattice structure of period 122 Å before detection by an Al tunnel junction. The filter resonance thus corresponds to a wavelength of about 240 Å and a frequency of about 2.2×10^{11} Hz. Figure 10 shows the observed transmission (points) as a function of phonon frequency; also shown are the corresponding phonon wavelengths. The solid line corresponds to the theoretically calculated filter function for an acoustical impedance ratio ($Z_1/Z_2 \approx 0.88$) and an overall line width of $\sim 0.2 \times 10^{11}$ Hz. Most of this line width arises from the width of the superconducting energy gap of the generator and detector used in these experiments. Experiments with superlattices with other periods show that the position of the resonance changes as expected with the superlattice period.

These results also show that phonons of wavelength ~ 100 Å suffer relatively little interface degradation even though they had to pass through 100 layers of the multilayered structure. This suggests that interfaces produced by MBE are nearly ideal, and one can think of using superlattice phonon mirrors as phonon spectrometers and for the manipulation of phonon diagnostic beams in semiconductors. Such mirrors can serve as the basis for the further development of phonon optics.

Conclusion

I have only briefly touched on some of the many exciting areas of phonon propagation research in semiconductors. Much has been learned about the details of phonon focusing, carrier relaxation and recombination, and phonon-defect interactions in several semiconductors. I have not had occasion in this article to discuss the great deal of work that has been done on the interaction of phonons with free carriers in degenerate semiconductors (*35, 36*) and on their role in determining many intriguing properties of e-h drops in germanium (*37*). A great deal of work still needs to be done. Study of phonon interactions with excitons, with layered two-dimensional (or even one-dimensional?) electron gases, and with novel superlattice structures is literally in its infancy. Interfaces prepared by MBE can serve as an ideal testing ground in determining the role of defects in interfacial degradation of phonons. The generation of large wave vector phonons in III-V semiconductors, using fundamental e-h recombination processes, needs to be applied to a variety of problems at short wavelengths. These include detailed mechanisms for anharmonic high-frequency phonon decay, energy states of donors and acceptors with small Bohr radii, the role of such phonons in determining recombination-enhanced defect migration in semiconductors, and the interaction of such phonons with electrons and holes in superlattices. Phonon microscopy at 10 Å in technologically important semiconductors appears feasible. Such studies are a powerful way of obtaining information on stress-sensitive properties on a truly atomic scale. Clearly much remains to be done in the area of phonon optics in semiconductors.

References and Notes

1. H. E. Bömmel and K. Dransfeld, *Phys. Rev.* **117**, 1245 (1960).
2. For a general text on the use of ultrasonic methods for studying crystalline materials, see A. S. Nowick and B. S. Berry, *Anelastic Relaxation in Crystalline Solids* (Academic Press, New York, 1972).
3. C. F. Quate, *Sci. Am.* **241**, 62 (October 1979).
4. J. Ilukor and E. H. Jacobsen, *Science* **153**, 1113 (1966).
5. R. J. Von Gutfeld, in *Physical Acoustics*, W. P. Mason, Ed. (Academic Press, New York, 1968), vol. 5, chap. 6.
6. W. Eisenmenger and A. H. Dayem, *Phys. Rev. Lett.* **18**, 125 (1967). For reviews, see W. Eisenmenger [in *Physical Acoustics*, W. P. Mason and R. N. Thurston, Eds. (Academic Press, New York, 1976), vol. 12, pp. 79–153] and W. E. Bron [*Rep. Prog. Phys.* **43**, 301 (1980)].
7. V. Narayanamurti, in *Proceedings of the NATO Advanced Study Institute on Nonequilibrium Superconductivity, Phonons and Kapitza Boundaries*, K. E. Gray, Ed. (Plenum, New York, 1981).
8. M. B. Panish, *Science* **208**, 916 (1980).
9. R. J. Von Gutfeld and A. H. Nethercot, Jr., *Phys. Rev. Lett.* **12**, 641 (1964); see also (*5*).
10. V. Narayanamurti, R. A. Logan, M. A. Chin, *Appl. Phys. Lett.* **33**, 481 (1978).
11. B. Taylor, H. J. Maris, C. Elbaum, *Phys. Rev. Lett.* **23**, 416 (1969).
12. M. J. P. Musgrave, *Proc. R. Soc. London Ser. A* **226**, 337 (1954); see also F. I. Federov, *Theory of Elastic Waves in Crystals* (Plenum, New York, 1968).
13. H. J. Maris, *J. Acoust. Soc. Am.* **50**, 812 (1971).
14. M. J. Lighthill, *Philos. Trans. R. Soc. London Ser. A* **252**, 397 (1960).
15. M. Lax and V. Narayanamurti, *Phys. Rev. B* **22**, 4876 (1980).
16. F. Rösch and O. Weis, *Z. Phys. B* **25**, 101 (1976).
17. J. C. Hensel and R. C. Dynes, *Phys. Rev. Lett.* **43**, 1033 (1979).
18. G. A. Northrup and J. P. Wolfe, *ibid.*, p. 1424.
19. W. Eisenmenger, in *Phonon Scattering in Condensed Matter*, H. J. Maris, Ed. (Plenum, New York, 1980), pp. 303–308.
20. M. Pomerantz and R. J. Von Gutfeld, in *Proceedings of the International Conference on the Physics of Semiconductors* (Nauka, Leningrad, 1968), vol. 2, p. 690.
21. R. C. Dynes and V. Narayanamurti, *Phys. Rev. B* **6**, 143 (1972).
22. W. Forkel, M. Welte, W. Eisenmenger, *Phys. Rev. Lett.* **31**, 215 (1973); see also (*6*).
23. V. Narayanamurti, R. A. Logan, M. A. Chin, *Phys. Rev. Lett.* **43**, 1536 (1979).
24. R. C. Dynes, V. Narayanamurti, M. A. Chin, *ibid.* **26**, 181 (1971).
25. D. V. Lang, R. A. Logan, M. Jaros, *Phys. Rev. B* **19**, 1015 (1979).
26. D. V. Lang, in "Proceedings of the 15th International Conference on the Physics of Semiconductors, Kyoto, 1980," *J. Phys. Soc. Jpn. Suppl. A* **49**, 215 (1980).
27. R. G. Ulbrich, in "Proceedings of the 14th International Conference on the Physics of Semiconductors, Edinburgh," *Inst. Phys. Conf. Ser. No. 43* (1978), p. 11.
28. R. G. Ulbrich, V. Narayanamurti, M. A. Chin, *Phys. Rev. Lett.* **45**, 1432 (1980).
29. J. T. Waugh and G. J. Dolling, *Phys. Rev.* **132**, 2410 (1963).
30. R. Orbach, *Phys. Rev. Lett.* **16**, 151 (1966); P. G. Klemens, *J. Appl. Phys.* **38**, 4573 (1967); H. J. Maris, *Phys. Lett.* **17**, 228 (1965); M. Lax, P. Hu, V. Narayanamurti, *Phys. Rev. B* **23**, 3095 (1981).
31. P. Hu, V. Narayanamurti, M. A. Chin, *Phys. Rev. Lett.* **46**, 192 (1981).
32. V. Narayanamurti, H. L. Stormer, M. A. Chin, A. C. Gossard, W. Wiegmann, *ibid.* **43**, 2012 (1979).
33. L. Brillouin, *Wave Propagation in Periodic Structures* (McGraw-Hill, New York, 1946).
34. M. Born and E. Wolf, *Principles of Optics* (Pergamon, New York, 1964).
35. J. P. Maneval, A. Zylberstejn, D. Huet, *Phys. Rev. Lett.* **27**, 1375 (1971); D. Huet and J. P. Maneval, *ibid.* **33**, 1159 (1974).
36. V. Narayanamurti, R. A. Logan, M. A. Chin, M. Lax, *Solid State Electron.* **21**, 1295 (1978).
37. J. C. Hensel and R. C. Dynes, *Phys. Rev. Lett.* **39**, 969 (1977).

38. I am indebted to several colleagues for discussions and for collaboration during the original parts of the work presented in this article. They include M. A. Chin, R. C. Dynes, R. C. Fulton, A. C. Gossard, P. Hu, M. Lax, R. A. Logan, H. L. Störmer, R. G. Ulbrich, and W. Wiegmann. Figures 4a and 4b were kindly supplied by Dr. J. C. Hensel and Prof. W. Eisenmenger, respectively.